

A novel perfluorocyclobutyl aryl ether-based graft copolymer via 2-methyl-1,4-bistrifluorovinyloxybenzene and styrene

Hao Liu^a, Sen Zhang^a, Yongjun Li^a, Dong Yang^{b,*}, Jianhua Hu^b, Xiaoyu Huang^{a,**}

^aKey Laboratory of Organofluorine Chemistry and Laboratory of Polymer Materials, Shanghai Institute of Organic Chemistry, Chinese Academy of Sciences, 345 Lingling Road, Shanghai 200032, PR China

^bKey Laboratory of Molecular Engineering of Polymers (Ministry of Education), Laboratory of Advanced Materials and Department of Macromolecular Science, Fudan University, 220 Handan Road, Shanghai 200433, PR China

ARTICLE INFO

Article history:

Received 21 June 2010

Received in revised form

13 August 2010

Accepted 27 August 2010

Available online 16 September 2010

Keywords:

ATRP

Graft copolymers

Perfluorocyclobutyl aryl ether

ABSTRACT

A series of novel perfluorocyclobutyl aryl ether-containing graft copolymers with polystyrene side chains were synthesized by the combination of thermal step-growth $[2\pi + 2\pi]$ cycloaddition polymerization of aryl bistrifluorovinyl ether monomer and atom transfer radical polymerization (ATRP) of styrene. We first synthesized a new aryl bistrifluorovinyl ether monomer of 2-methyl-1,4-bistrifluorovinyloxybenzene in two steps using commercially available 2-methylhydroquinone as starting material and the corresponding perfluorocyclobutyl aryl ether-based homopolymer with methoxyl end groups was prepared through the homopolymerization of this monomer in diphenyl ether. Next, the pendant methyls of this fluoropolymer were mono-brominated by *N*-bromosuccinimide and benzoyl peroxide so as to be converted to ATRP initiation groups. The targeted poly(2-methyl-1,4-bistrifluorovinyloxybenzene)-*g*-polystyrene with relatively narrow molecular weight distributions ($M_w/M_n \leq 1.38$) was obtained by the combination of bulk ATRP of styrene at 110 °C using CuBr/bpy as catalytic system and the grafting-from strategy. These fluorine-containing graft copolymers show excellent solubility in common organic solvents.

© 2010 Elsevier Ltd. All rights reserved.

1. Introduction

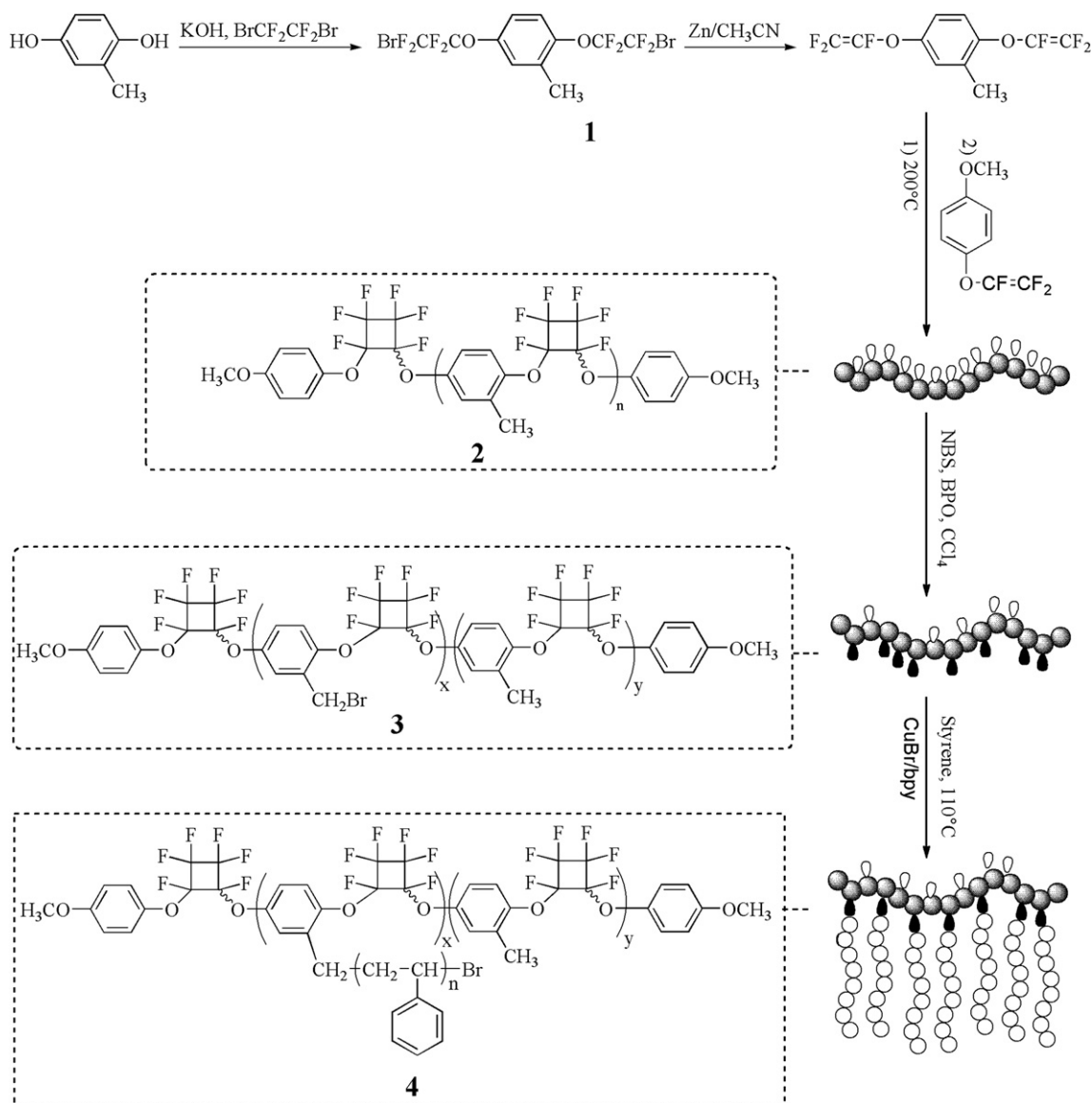
Since the first example of fluoropolymer, polytetrafluoroethylene (PTFE), was discovered by Dr. Plunkett of DuPont in 1938 [1], many different kinds of high-performance fluoropolymers have been developed and applied in different fields because of their excellent properties, such as high thermal and oxidative stability, high chemical resistance, low surface energy, optical transparency and high insulating ability [2], which originated from the incorporation of fluorocarbon functionality. However, the high crystallinity of fluoropolymers led to low solubility and processability so that the extensive applications of fluoropolymers have been obviously limited [2]. Therefore, partially fluorinated polymers with good solubility including polychlorotrifluoroethylene (PCTFE), Teflon-AF, Cytop and various copolymers of PTFE have been synthesized to meet the application needs [2].

* Corresponding author. Tel.: +86 21 55665280; fax: +86 21 65640293.

** Corresponding author. Tel.: +86 21 54925310; fax: +86 21 64166128.

E-mail addresses: yangdong@fudan.edu.cn (D. Yang), xyhuang@mail.sioc.ac.cn (X. Huang).

In 1993, perfluorocyclobutyl (PFCB) aryl ether polymer, a relatively new partially fluorinated polymer, was first obtained by Babb *et al.* of Dow Chemical Co. [3,4]. This fluoropolymer was prepared by the predominant head-to-head thermal $[2\pi + 2\pi]$ step-growth cyclopolymerization of aryl trifluorovinyl ethers (TFVE) at temperature of 150–200 °C in bulk or solution without any initiator and catalyst. Many kinds of new thermoplastic and thermoset PFCB aryl ether polymers have been synthesized by the thermal chain extension of bis- and tri-functionalized TFVE monomers [5–9]. PFCB aryl ether-based polymers which have demonstrated entirely amorphous not only have the common properties of fluoropolymer such as high thermal/oxidative stability, high chemical resistance, low dielectric constant, low moisture absorption and low surface energy, but show many other advantages like optical transparency and improved processability [10,11] due to the combination of flexible thermally robust, aromatic ethers with fluorocarbon linkage. Furthermore, the substitution groups of bis- or tri-phenol block can be changed to afford many new PFCB aryl ether-based polymers tailored for a variety of applications, such as optical waveguide applications [10,12,13], proton exchange membrane [14], hole-transporting material [15,16], curing additive [17] and space durable materials [18,19].



Scheme 1. Synthesis of PMBTFVB-g-PS graft copolymer.

Until now, the majority of PFCB aryl ether-based polymer-concerned researches focused on the homopolymerization and random copolymerization of different TFVE monomers due to very high polymerization temperature ($>150\text{ }^{\circ}\text{C}$) and unusual radical-mediated $[2\pi + 2\pi]$ cyclopolymerization mechanism [20], which apparently confined its development as an emerging class of semi-fluorinated polymer. For enlarging its application range, it is significant to combine the high performance of PFCB aryl ether polymer with other commercial polymers. Block and graft copolymers with a stable covalent-bonded linkage between two different segments may be a good choice. Recently, some groups have synthesized the block copolymers containing PFCB aryl ether segment [21–24]; however, PFCB aryl ether-based graft polymer has never been reported until now.

Generally, three strategies of grafting-through, grafting-onto and grafting-from are employed for synthesizing the graft polymers [25]. Graft polymers can be obtained by the homopolymerization or copolymerization of the macromonomers through the grafting-through method. But, the conventional free radical

polymerization of the macromonomers yielded the graft copolymers with a broad chain-length distribution [26] and well-defined graft copolymers with low molecular weights were obtained by the living polymerization of the macromonomers [27]. The grafting-onto approach of grafting the side chains onto the backbone by a coupling reaction with a high coupling efficiency is suitable for the synthesis of graft copolymers possessing short side chains [28,29]. The grafting-from technology utilizes the pendant initiation sites on the backbone introduced from the initiation-group-containing monomer or by the post-modification of the backbone to initiate the polymerization of another monomer to form the side chains [30]. A variety of well-defined graft polymers have been synthesized by living radical polymerization such as atom transfer radical polymerization (ATRP) [31–33], modified ATRP [34,35], single-electron-transfer living radical polymerization (SET-LRP) [36,37], reversible addition fragmentation chain transfer (RAFT) polymerization [38,39] via the grafting-from strategy. In particular, the living nature of ATRP enabled it to form the side chains in a well-defined way with controllable molecular weights and polydispersities [30,40–42].

In this article, we reported a novel PFCB aryl ether-based graft polymer bearing polystyrene (PS) side chains. A new aryl bistrifluorovinyl ether monomer, 2-methyl-1,4-bistrifluorovinylbenzene (MBTVFB), was first homopolymerized at 200 °C to provide PFCB aryl ether-based backbone. The homopolymer was transformed into ATRP macroinitiator via the mono-bromination of the pendant methyls. The final graft copolymer, poly(2-methyl-1,4-bistrifluorovinylbenzene)-*g*-polystyrene (PMBTFVB-*g*-PS), was obtained via ATRP graft copolymerization of styrene.

2. Experimental section

2.1. Materials

Styrene (St, Aldrich, 99%) was washed with 5% aqueous NaOH solution to remove the inhibitor and then with water, dried over MgSO₄, and distilled twice from CaH₂ under reduced pressure prior to use. CuBr (Aldrich, 98%) was purified by stirring overnight over CH₃CO₂H at room temperature, followed by washing the solid with ethanol, diethyl ether, and acetone prior to drying *in vacuo* at 40 °C for 1 day. Granular zinc (Aldrich, 99.99%) was activated by washing in 0.1 M HCl followed by drying *in vacuo* at 140 °C for 10 h. Toluene (Aldrich, 99%) was dried over CaH₂ and distilled from sodium and benzophenone under N₂ prior to use. Anisole (Aldrich, 99%) and diphenyl ether (Aldrich, 99%) were dried over CaH₂ and distilled under reduced pressure prior to use. *N*-Bromosuccinimide (NBS, Aldrich, 99%) was recrystallized from water and dried *in vacuo* at 35 °C for 1 day. Benzoyl peroxide (BPO, Alfa Aesar, 97%) was purified by dissolving in acetone and precipitating in water followed by drying *in vacuo* at room temperature for 1 day. BrCF₂CF₂Br was prepared by condensing equimolar amounts of Br₂ and tetrafluoroethylene at –195 °C followed by warming up to 22 °C [43]. 4-Methoxytrifluorovinylbenzene was prepared according to previous literature [44]. CH₃CN (Aldrich, 99.8%), CCl₄ (Aldrich, 99.5%), dimethyl sulfoxide (DMSO, Aldrich, 99.9%), KOH (Aldrich, 90%), 2,2'-bipyridine (bpy, Aldrich, 99%) and 2-methylhydroquinone (Aldrich, 99%) were used as received.

2.2. Measurements

FT-IR spectra were recorded on a Nicolet AVATAR-360 FT-IR spectrophotometer with a resolution of 4 cm⁻¹. All NMR analyses were performed on a Bruker AM-300 spectrometer (300 MHz) in CDCl₃, TMS (¹H NMR) and CDCl₃ (¹³C NMR) were used as internal standards and CF₃CO₂H was used as external standard for ¹⁹F NMR. EI-MS and HRMS were measured by an Agilent 5937N system and a Waters Micromass GCT instrument, respectively. The bromine content was determined by the titration with Hg(NO₃)₂. Relative molecular weights and molecular weight distributions were measured by conventional gel permeation chromatography (GPC) system equipped with a Waters 1515 Isocratic HPLC pump, a Waters 2414 refractive index detector, and a set of Waters Styragel columns (HR3 (500–30,000), HR4 (5000–600,000) and HR5 (50,000–4,000,000), 7.8 × 300 mm, particle size: 5 μm). GPC measurements were carried out at 35 °C using tetrahydrofuran (THF) as eluent with a flow rate of 1.0 mL/min. The system was calibrated with linear polystyrene standards. Conversions of St were determined by GC using an HP 6890 system with an SE-54 column and anisole was used as internal standard. Differential scanning calorimetry (DSC) measurements were run on a TA Q200 system under N₂ purge with a heating rate of 10 °C/min. The glass transition temperature (*T*_g) was recorded from the second heating process after a quick cooling from 200 °C and the value was determined from the midpoint of *C*_p curve. Thermo-gravimetric analysis (TGA) measurements were run on a TA Q500 system under

N₂ purge with a heating rate of 10 °C/min. The decomposition temperature (*T*_d) is defined as the temperature with 10% weight loss.

2.3. Synthesis of MBTFVB

2-Methylhydroquinone was used as starting material to synthesize MBTVFB **1** monomer in two steps as shown in Scheme 1. To a 500 mL three-neck flask (flame-dried prior to use) fitted with a N₂ inlet and a Barrett trap topped with a reflux condenser, 2-methylhydroquinone (12.41 g, 0.10 mol), toluene (120 mL) and DMSO (150 mL) were first added followed by deoxygenating under N₂ for 30 min. Next, KOH (12.44 g, 90%, 0.20 mol) was added and the mixture was refluxed at 180 °C to azeotropically remove the water until no more water was collected in the trap. The solution was then cooled to below 15 °C and BrCF₂CF₂Br (30 mL, 0.25 mol) was introduced dropwise within 1 h. The mixture was warmed to room temperature for 12 h and heated to 35 °C for another 8 h. The reaction was quenched by water and the mixture was extracted with CH₂Cl₂. All organic layers were collected and dried over MgSO₄. 2-Methyl-1,4-bis(2-bromotetrafluoroethoxy)phenyl (19.76 g, 40.9%) as clear oil was obtained by silica column chromatography. ¹H NMR (300 MHz, CDCl₃): δ (ppm): 2.24 (3H, CH₃), 7.08, 7.13, 7.24 (3H, phenyl). HRMS: C₁₁H₆O₂Br₂F₈, calcd 479.8607, found 479.8604.

To a 250 mL three-neck flask (flame-dried prior to use) fitted with a reflux condenser, zinc (11.44 g, 0.176 mmol) was first added followed by three cycles of evacuating and backfilling with N₂. CH₃CN (120 mL) was introduced via a gastight syringe and the mixture was refluxed at 110 °C. The above prepared intermediate, 2-methyl-1,4-bis(2-bromotetrafluoroethoxy)phenyl (24.19 g, 0.05 mmol) was added dropwise within 1 h and the mixture was refluxed at 110 °C for 10 h. After cooling to room temperature, the suspending zinc salt was removed by the filtration and the filtrate was washed with water and dried over MgSO₄. The crude product was purified by silica column chromatography to afford 9.20 g (65.0%) of MBTFVB **1** as clear oil. FT-IR: ν (cm⁻¹): 3045, 2968, 1833, 1600, 1496, 1422, 1315, 1279, 1179, 1157, 1009, 945, 874, 808, 767. ¹H NMR (300 MHz, CDCl₃): δ (ppm): 2.33 (s, 3H, CH₃), 6.93 (d, *J* = 8.8 Hz, 1H, phenyl), 6.97 (s, 1H, phenyl), 7.01 (d, *J* = 8.8 Hz, 1H, phenyl). ¹³C NMR (75 MHz, CDCl₃): δ (ppm): 15.7 (CH₃), 114.3, 115.5, 119.0, 129.9 (phenyl), 132.8, 135.2, 143.9, 144.4, 146.5, 147.1, 149.3, 149.9 (OCF=CF₂), 150.3, 151.6 (phenyl). ¹⁹F NMR (282 MHz, CDCl₃): δ (ppm): –120.3, –127.0, –134.3. EI-MS: *m/z* (%): 284 ([M]⁺, 100.00), 187 (20.49), 159 (11.81), 140 (24.04), 119 (17.50), 109 (32.77), 90 (83.16), 77 (4.09), 51 (7.58). HRMS: C₁₁H₆O₂F₆: calcd 284.0272, found, 284.0268.

2.4. Thermal homopolymerization of MBTFVB

PMBTFVB **2** homopolymer was prepared by the thermal step-growth cyclo-addition polymerization of MBTFVB **1** monomer. To a 50 mL Schlenk flask (flame-dried under vacuum prior to use) sealed with a rubber septum, MBTFVB **1** (8.00 g, 28.16 mmol) and diphenyl ether (16 mL) were first added under N₂. The flask was degassed by three cycles of freezing–pumping–thawing followed by immersing the flask into an oil bath thermostated at 200 °C. 4-Methoxytrifluorovinylbenzene (2.87 g, 14.07 mmol) was introduced via a gastight syringe after 4 h. The polymerization was terminated by putting the flask into liquid N₂ after another 6 h. THF (15 mL) was added to dilute the solution followed by precipitating into methanol. After repeated purification by dissolving in THF and precipitating in methanol, PMBTFVB **2** homopolymer (4.53 g, 56.6%) as white powder was obtained after drying *in vacuo* overnight. GPC: *M*_n = 4600 g/mol, *M*_w/*M*_n = 1.27. FT-IR: ν (cm⁻¹): 3053,

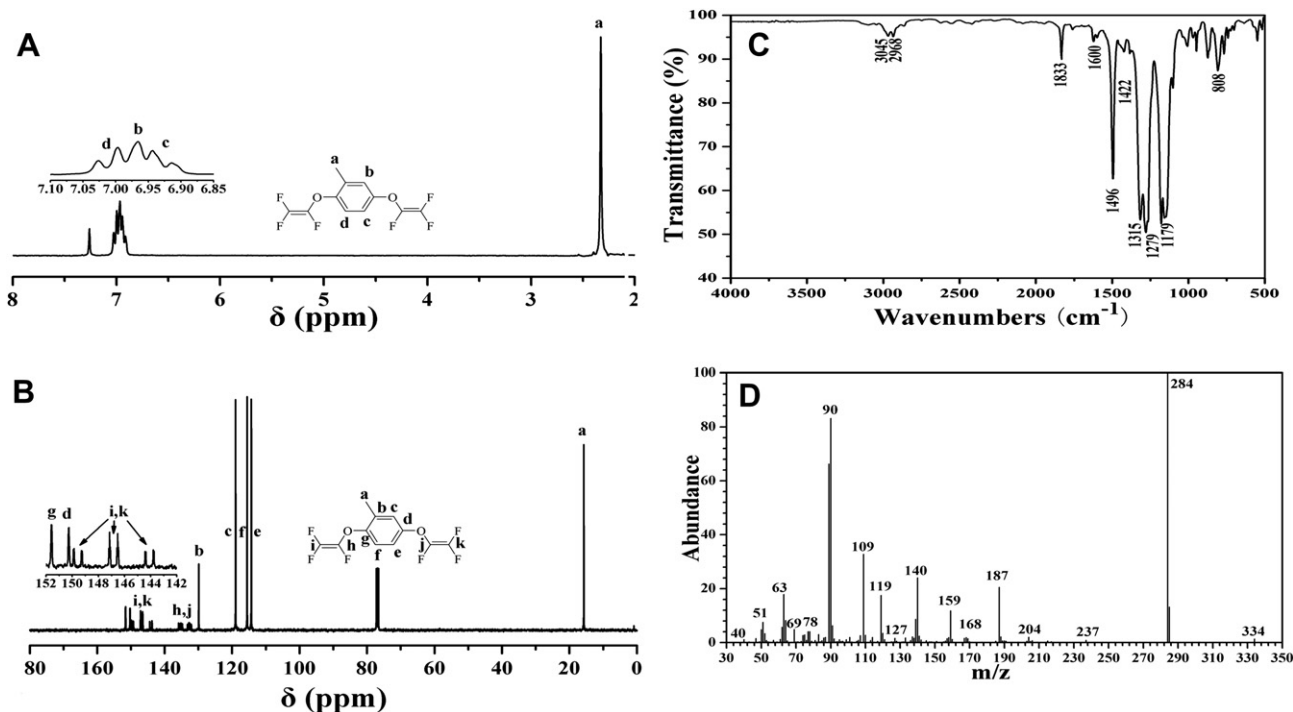


Fig. 1. ^1H NMR (A), ^{13}C NMR (B), FT-IR (C), and EI-MS (D) spectra of MBTVFB 1.

2933, 1599, 1498, 1315, 1267, 1203, 1120, 1009, 962, 925, 813, 743. ^1H NMR (300 MHz, CDCl_3): δ (ppm): 2.06, 2.27 (3H, CH_3), 3.77 (3H, OCH_3), 6.97, 7.10 (3H, phenyl). ^{13}C NMR (75 MHz, CDCl_3): δ (ppm): 16.0 (CH_3), 55.4 (OCH_3), 105.7, 109.2, 112.7 (4C, PFCB), 116.5, 121.5, 131.0, 148.3 (phenyl). ^{19}F NMR (282 MHz, CDCl_3): δ (ppm): -128.3 to -132.2 (6F, PFCB).

2.5. Mono-bromination of PMBTFBV

NBS and BPO were used to mono-brominate the pendant methyls of PMBTFBV **2** homopolymer. In a typical procedure, PMBTFBV **2** ($M_n = 4600$ g/mol, $M_w/M_n = 1.27$, 2.00 g, 7.04 mmol CH_3 group), NBS (1.2530 g, 7.04 mmol), and BPO (0.3415 g, 1.41 mmol) were first added to a 1000 mL three-neck flask (flame-dried prior to use) fitted with a reflux condenser and the solution was deoxygenated under N_2 . Next, CCl_4 (400 mL) was introduced via a gastight syringe and the solution was refluxed at 80°C for 1 day. After filtration, CCl_4 was removed from the filtrate using a rotary evaporator. The obtained solid was dissolved in 500 mL of ethyl acetate and the resulting solution was washed with distilled water (200 mL \times 2) followed by drying over MgSO_4 . The solution was concentrated and precipitated into methanol. After repeated purification by dissolving in THF and precipitating in methanol, 1.0792 g of PMBTFBV-Br **3b** macroinitiator as white powder was obtained after drying *in vacuo* overnight. GPC: $M_n = 6200$ g/mol, $M_w/M_n = 1.14$. EA: Br%: 16.28%. ^1H NMR (300 MHz, CDCl_3): δ (ppm): 1.99, 2.18 (3H, CH_3), 3.68 (3H, OCH_3), 4.17, 4.34 (2H, CH_2Br), 6.86, 7.04, 7.16 (3H, phenyl). ^{13}C NMR (75 MHz, CDCl_3): δ (ppm): 15.3 (CH_3), 24.6 (CH_2Br), 54.7 (OCH_3), 105.0, 107.8, 111.7 (4C, PFCB), 116.5, 118.7, 120.8, 129.3, 148.1 (phenyl). ^{19}F NMR (282 MHz, CDCl_3): δ (ppm): -127.1 to -132.7 (6F, PFCB).

2.6. ATRP graft copolymerization of St

ATRP bulk graft copolymerization of St was performed by using PMBTFBV-Br **3** as macroinitiator and CuBr/bpy as catalytic system.

ATRP macroinitiator **3**, CuBr and bpy were first added to a 25 mL Schlenk flask (flame-dried under vacuum prior to use) sealed with a rubber septum under N_2 . After three cycles of evacuating and purging with N_2 , St was charged via a gastight syringe. The flask was degassed by three cycles of freezing–pumping–thawing followed by immersing the flask into an oil bath preset at 110°C . The polymerization was terminated by immersing the flask into liquid N_2 after certain time. The reaction mixture was diluted with THF and passed through an alumina column to remove the residual copper catalyst. The solution was concentrated and precipitated into methanol. After repeated purification by dissolving in THF and precipitating in methanol, PMBTFBV-g-PS **4** graft copolymer as white powder was obtained after drying *in vacuo* overnight. FT-IR: ν (cm^{-1}): 3060, 3026, 2923, 2851, 1600, 1492, 1452, 1315, 1262, 1204, 1111, 1028, 961, 756, 698. ^1H NMR (300 MHz, CDCl_3): δ (ppm): 1.43 (2H, CHCH_2), 1.86 (1H, CHCH_2), 2.04 (3H, CH_2 connected to the aryl), 2.25 (3H, CH_3), 3.73 (3H, OCH_3), 4.41, 4.49 (1H, CHBr), 6.59, 7.09 (3H, phenyl of the backbone; 5H, phenyl of PS side chain). ^{19}F NMR (282 MHz, CDCl_3): δ (ppm): -128.4 to -131.9 (6F, PFCB). ATRP kinetics was investigated by using PMBTFBV-Br **3a** macroinitiator and anisole ($V_{\text{anisole}}:V_{\text{St}} = 1:20$) was added as internal standard for GC measurement.

3. Results and discussion

3.1. Synthesis of MBTVFB aryl bistrifluorovinyl ether monomer

MBTVFB **1** aryl bistrifluorovinyl ether monomer was synthesized according to standard procedures of the fluoroalkylation with $\text{BrCF}_2\text{CF}_2\text{Br}$ and Zn-mediated elimination in two steps with a total yield of 26.6% using commercially available 2-methylhydroquinone as starting material [18,20,45]. The chemical structure of this monomer was examined by FT-IR, EI-MS, HRMS, ^1H NMR, ^{19}F NMR and ^{13}C NMR. ^1H NMR spectrum of MBTVFB **1** is shown in Fig. 1A and the typical resonance signal of the methyl appeared at 2.33 ppm. A series of peaks around 7.00 ppm belonged to 3 protons

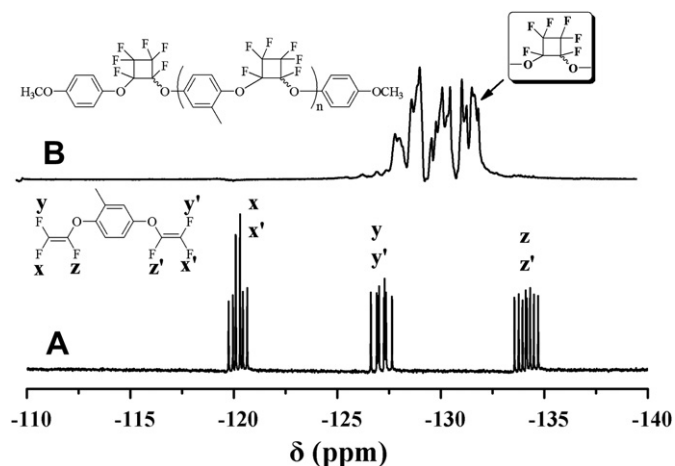


Fig. 2. ^{19}F NMR spectra of MBTFVB **1** (A) and PMBTFVB **2** (B).

of the benzene ring. The singlet at 6.97 ppm is attributed to 1 proton adjacent to the methyl. Another 2 doublets at 6.93 and 7.01 ppm originated from other 2 protons of benzene ring. The peaks ranging from 132.8 ppm to 149.9 ppm in ^{13}C NMR spectrum of MBTFVB **1** (Fig. 1B) corresponded to 2 carbons of the trifluorovinyl [18,46]. The signal of the methyl located at 15.7 ppm and the peaks at 114.3, 115.5, 119.0, 129.9, 150.3 and 151.6 ppm belonged to 6 carbons of the benzene ring [18,46]. In addition, three typical multiplets at -120.3 , -127.0 and -134.3 ppm [18,46] in ^{19}F NMR spectrum (Fig. 2A) showed the existence of the trifluorovinyl. Fig. 1C shows FT-IR spectrum of MBTFVB **1** and the typical peak of the trifluorovinyl was found to be located at 1833 cm^{-1} . The signals of the benzene ring and the ether bond appeared at 1600 , 1496 , 808 and 1179 cm^{-1} , respectively. EI-MS spectrum of MBTFVB **1** is shown in Fig. 1D and the peak of m/z 284 corresponded to the molecular ion peak of MBTFVB **1**. Moreover, HRMS provided the formula of $\text{C}_{11}\text{H}_6\text{O}_2\text{F}_6$ and the found mass was 284.0268 , which is almost equal to the calculated mass of 284.0272 . Therefore, all these evidences confirmed the successful synthesis of bistrifluorovinyl-containing monomer **1**.

3.2. Preparation of PMBTFVB homopolymer

PMBTFVB **2** homopolymer was obtained via thermal $[2\pi + 2\pi]$ step-growth cycloaddition polymerization of bifunctional MBTFVB **1** monomer in diphenyl ether at $200\text{ }^\circ\text{C}$ and both ends of the homopolymer were capped by mono-functional 4-methoxytrifluorovinylbenzene. FT-IR, ^1H NMR, ^{13}C NMR and ^{19}F NMR were employed to characterize this homopolymer. FT-IR spectrum after thermal homopolymerization (Fig. 3A) showed the complete disappearance of the typical signal of the trifluorovinyl at 1833 cm^{-1} and a new sharp peak of PFCB linkage appeared at 962 cm^{-1} in Fig. 3A compared to that of the monomer (Fig. 1C), thus indicating the existence of PFCB linkage in the homopolymer. Moreover, the representative signals of the trifluorovinyl in ^{19}F NMR spectrum disappeared after thermal homopolymerization (Fig. 2B) and new multiplets in the range between -128.3 ppm and -132.2 ppm appeared instead, which also demonstrated the presence of PFCB functionality. The singlets at 2.06 and 2.27 ppm in ^1H NMR spectrum after thermal homopolymerization (Fig. 4A) belonged to 3 protons of the methyl and the broad peaks at 6.97 and 7.10 ppm were attributed to 3 protons of the benzene ring. The signal of 3 protons of terminal methoxyl clearly appeared at 3.77 ppm as a singlet, which confirmed the effective end-capping

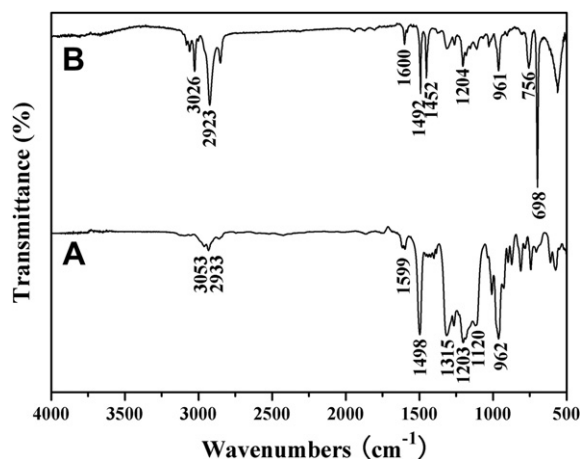


Fig. 3. FT-IR spectra of PMBTFVB **2** (A) and PMBTFVB-g-PS **4** (B).

with 4-methoxytrifluorovinylbenzene. The disappearance of the signals of the trifluorovinyl was also illustrated by ^{13}C NMR spectrum after thermal homopolymerization (Fig. 4B) in comparison with that of the monomer (Fig. 1B). Instead, new peaks originated from 4 carbons of PFCB linkage were found to be located in the area ranging from 106.5 ppm to 112.7 ppm. Another new peak at 55.4 ppm was attributed to the carbon of terminal methoxyl.

The relative molecular weight of PMBTFVB **2** ($M_n = 4600\text{ g/mol}$) was obtained by GPC measurement calibrated with linear polystyrene standards and ^1H NMR was employed to determine the 'absolute' molecular weight of the homopolymer. The molecular weight of PMBTFVB **2** ($M_{n,\text{NMR}}$) can be evaluated according to Eq. (1) (S_a and S_b are the area of peak 'a' at 3.77 ppm and peaks 'b' at 2.06 and 2.27 ppm in Fig. 4A, respectively; 284 and 204 are the molecular weights of MBTFVB **1** monomer and 4-methoxytrifluorovinylbenzene). The value of S_b/S_a is 15.5 and the molecular weight is calculated to be 9200 g/mol . This result indicates that every PMBTFVB **2** chain possesses 31.0 ($=15.5 \times 2$) repeating units.

$$M_{n,\text{NMR}} = 284 \times (2S_b/S_a) + 204 \times 2 \quad (1)$$

Thus, all the above results verified the structure of PMBTFVB **2** homopolymer. In addition, this homopolymer can dissolve in most

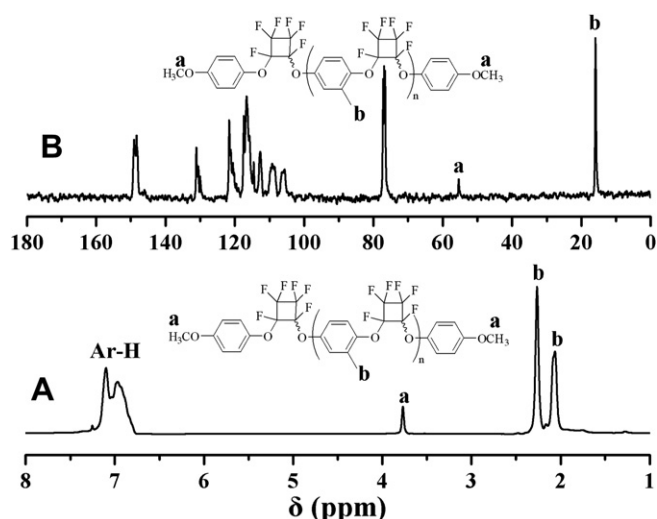


Fig. 4. ^1H NMR (A) and ^{13}C NMR (B) spectra of PMBTFVB **2** in CDCl_3 .

Table 1
Preparation of PMBTFVB–Br **3** macroinitiator.^a

Sample	NBS (equiv)	Br% ^b (%)	$M_{n,GPC}$ ^c (kDa)	M_w/M_n ^c	$M_{n,NMR}$ ^d (kDa)	N_{ATRP} ^e	D_{ATRP} ^f (%)
3a	0.7	12.34	5.7	1.18	10.4	16.2	52.3
3b	1.0	16.28	6.2	1.14	10.8	22.3	71.9

^a Reaction temperature: 80 °C; reaction time: 24 h; feeding ratio: [methyl]: [BPO] = 1:0.2.

^b Determined by the titration with $Hg(NO_3)_2$.

^c Measured by GPC in THF at 35 °C.

^d Determined by 1H NMR.

^e The number of ATRP initiation group per chain.

^f Grafting density of ATRP initiation group.

common organic solvents including THF, CH_2Cl_2 , chloroform, hexane, cyclohexane, toluene, acetone, ethyl acetate and DMF; however, it can't dissolve in water and methanol.

3.3. Transformation of PMBTFVB into Br-containing ATRP macroinitiator

Mono-bromination of the pendant methyls of PMBTFVB **2** homopolymer was conducted in CCl_4 by reacting with NBS and BPO so that the homopolymer was converted to PMBTFVB–Br **3** macroinitiator. Two different feeding ratios of NBS to the methyls have been used to adjust the degree of bromination and it was found that adding more NBS led to the raising of the bromine content as listed in Table 1. After the reaction with NBS and BPO, the bromine contents of both samples increased from 0% to 12.34% for **3a** and 16.28% for **3b** (Table 1), respectively, this obviously indicating the presence of Br-containing ATRP initiation sites in both samples [47,48]. The molecular weights of both samples after the reaction with NBS and BPO ($M_{n,GPC}$ in Table 1) were higher than that of PMBTFVB **2** homopolymer ($M_{n,GPC} = 4600$ g/mol), which also evidenced the occurrence of the bromination reaction.

1H NMR spectrum after the reaction (Fig. 5A) shows the appearance of two new peaks at 4.17 and 4.34 ppm, which corresponded to 2 protons of newly formed CH_2Br group. A new peak attributed to the carbon of CH_2Br group also appeared at 24.6 ppm in ^{13}C NMR spectrum after the reaction (Fig. 5B). In addition, the remaining of the original signals of PMBTFVB **2** homopolymer in 1H NMR (Fig. 5A), ^{13}C NMR (Fig. 5B) and ^{19}F NMR spectra after the reaction demonstrated

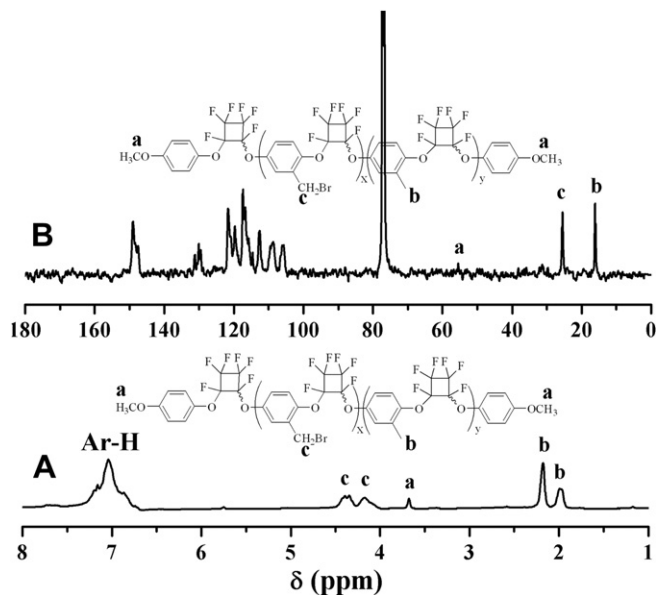


Fig. 5. 1H NMR (A) and ^{13}C NMR (B) spectra of PMBTFVB–Br **3** in $CDCl_3$.

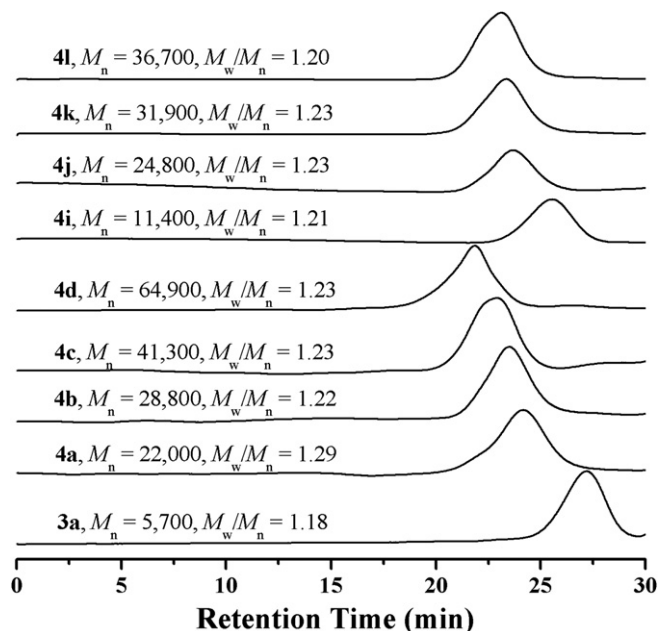


Fig. 6. GPC traces of PMBTFVB–Br **3** and PMBTFVB-g-PS **4** in THF.

that the polymeric architecture was kept during the reaction. Fig. 6 shows a unimodal and symmetrical GPC curve for PMBTFVB–Br **3a**, which also verified that the architecture of polymer chain was not altered during the bromination [49]. These results also confirmed the successful mono-bromination of PMBTFVB **2** homopolymer without affecting the polymeric backbone.

The number of CH_2Br ATRP initiation group (N_{ATRP}) can be estimated via the data of Br% (Table 1) according to the following equation set, ('x' and 'y' are the numbers of repeating unit with CH_2Br and CH_3 group as shown in Scheme 1; 204 and 80 are the molecular weights of 4-methoxytrifluorovinyloxybenzene and bromine atom; 363 and 284 are the molecular weights of repeating unit with CH_2Br and CH_3 group; 31.0 is the number of repeating unit of PMBTFVB **2** homopolymer). The values of N_{ATRP} for PMBTFVB–Br **3a** and **3b** are calculated to be 16.2 and 22.3, respectively. Thus, the grafting densities of CH_2Br ATRP initiation group (D_{ATRP}) are 52.3% = 16.2/31.0 and 71.9% = 22.3/31.0 for **3a** and **3b** macroinitiators as listed in Table 1, respectively.

$$\begin{cases} \frac{80x}{363x + 284y + 204 \times 2} = Br\% & (2) \\ x + y = 31.0 & (3) \end{cases}$$

The molecular weights of PMBTFVB–Br **3** macroinitiators ($M_{n,NMR}$) were determined by 1H NMR according to Eq. (4), in which S_a , S_b and S_c are the area of peak 'a' at 3.68 ppm, peaks 'b' at 1.99 and 2.18 ppm and peaks 'c' at 4.17 and 4.34 ppm in Fig. 5A, respectively. The values are 10,400 g/mol for PMBTFVB–Br **3a** and 10,800 g/mol for PMBTFVB–Br **3b** as listed in Table 1, respectively.

$$M_{n,NMR} = 363 \times (3S_c/S_a) + 284 \times (2S_b/S_a) + 204 \times 2 \quad (4)$$

Therefore, we can conclude that bromine-containing ATRP initiation sites have been successfully introduced into the main chain without affecting the polymeric architecture, and 16.2 and

Table 2
Synthesis of PMBTFVB-g-PS **4** graft copolymer.^a

Sample	Time (h)	$M_{n,GPC}^d$ (kDa)	M_w/M_n^d	N_{St}^e	n_{St}^f	$M_{n,NMR}^g$ (kDa)
4a ^b	1.5	22.0	1.29	247.9	15.3	36.2
4b ^b	3	28.8	1.22	367.7	22.7	48.6
4c ^b	5	41.3	1.23	453.6	28.0	57.6
4d ^b	7	64.9	1.23	831.1	51.3	96.8
4e ^c	1.5	31.7	1.33	278.8	12.5	39.8
4f ^c	3	47.6	1.38	533.0	23.9	66.2
4g ^c	5	67.5	1.28	967.8	43.4	111.5
4h ^c	7	98.6	1.34	1179.7	52.9	133.5

^a Polymerization temperature: 110 °C; feeding ratio: [St]:[CH₂Br group]:[CuBr]:[bpy] = 400:1:1:2.

^b Initiated by PMBTFVB–Br **3a**.

^c Initiated by PMBTFVB–Br **3b**.

^d Measured by GPC in THF at 35 °C.

^e Total number of St repeating unit obtained from ¹H NMR.

^f The number of St repeating unit per PS side chain obtained from ¹H NMR.

^g Determined by ¹H NMR.

22.3 CH₂Br groups are involved in PMBTFVB–Br **3a** and **3b** macroinitiators, respectively.

3.4. Synthesis of PMBTFVB-g-PS graft copolymer

ATRP of St was initiated by PMBTFVB–Br **3** macroinitiator at 110 °C using CuBr/bpy as catalytic system to yield PMBTFVB-g-PS **4** graft copolymers via the grafting-from strategy and the results are summarized in Table 2. It was found that the molecular weights of the obtained graft copolymers were all much higher than those of the macroinitiators, which indicated ATRP of St was performed. The molecular weights of graft copolymers also increased with the extending of polymerization time, which accorded with the characteristic of ATRP [31]. In this case, the intermolecular coupling reactions were suppressed by the combination of a high feeding ratio of St to CH₂Br initiation group (400:1) and a relatively low conversion of St (<15%) according to previous reports [47–55]. All graft copolymers showed unimodal and symmetrical GPC curves (Fig. 6) with relatively narrow molecular weight distributions ($M_w/M_n \leq 1.38$), which confirmed that intermolecular coupling reactions could be neglected [52].

Fig. 3B shows FT-IR spectrum of PMBTFVB-g-PS **4** graft copolymer and the typical signal of perfluorocyclobutyl unit located at 961 cm⁻¹. The bands at 3026, 1600, 1492 and 1452 cm⁻¹ originated from the benzene ring of PMBTFVB backbone and PS side chains. In particular, two sharp peaks at 756 and 698 cm⁻¹ witnessed the existence of mono-substituted benzene ring in PS side chains. All characteristic ¹H NMR signals of the corresponding protons of PMBTFVB backbone and PS side chains appeared in ¹H NMR spectrum after graft copolymerization (Fig. 7A). The strong peaks at 1.43 and 1.86 ppm were attributed to 2 protons of CH₂ group and 1 proton of CH group of PS side chains, respectively. Fig. 7A also shows the disappearance of the signals of 2 protons of CH₂Br initiation group connected to the benzene ring which appeared at 4.17 and 4.34 ppm in Fig. 5A, thus indicating the complete involvement of every pendant ATRP initiation group in graft polymerization of St. Furthermore, two minor peaks corresponding to CHBr end group of PS side chain were found to be located at 4.41 and 4.49 ppm, which demonstrated ATRP mechanism of graft copolymerization of St [56]. The signal of 3 protons of terminal methoxyl of the backbone remained at 3.73 ppm after copolymerization. The presence of PFCB linkage in PMBTFVB-g-PS **4** graft copolymer was also verified by a series of peaks between –128.4 and –131.9 ppm in ¹⁹F NMR spectrum after copolymerization (Fig. 7B). Therefore, all these evidences confirmed the structure of PMBTFVB-g-PS **4** graft copolymer.

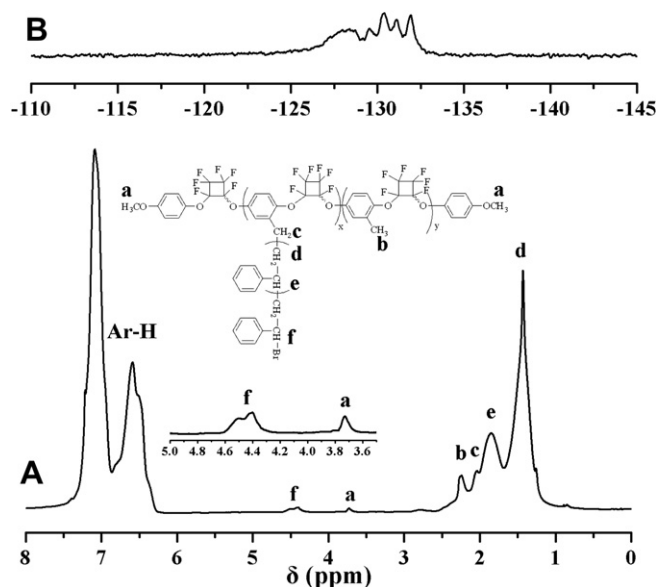


Fig. 7. ¹H (A) and ¹⁹F (B) NMR spectra of PMBTFVB-g-PS **4** in CDCl₃.

Since the molecular weight of the graft copolymer measured by GPC is much lower than the ‘real’ value [57], we used ¹H NMR to determine the molecular weight of PMBTFVB-g-PS **4** graft copolymer ($M_{n,NMR}$) instead of GPC. The total number of St repeating unit (N_{St}), the molecular weight of the graft copolymer ($M_{n,NMR}$) and the number of St repeating unit per PS side chain (n_{St}) were calculated according to Eq. (5) (S_d and S_a are the area of peak ‘d’ at 1.43 ppm and peak ‘a’ at 3.73 ppm in Fig. 7A, respectively), Eq. (6) ($M_{n,3}$ is the molecular weight of PMBTFVB–Br **3** macroinitiator as listed in Table 1 and 104 is the molecular weight of St) and Eq. (7) (N_{ATRP} is the number of grafted ATRP initiation group per chain as listed in Table 1), respectively. The molecular weights obtained from ¹H NMR (Table 2) are actually much higher than those measured by GPC.

$$N_{St} = 3 \times (S_d/S_a) \quad (5)$$

$$M_{n,NMR} = M_{n,3} + 104 \times N_{St} \quad (6)$$

$$n_{St} = N_{St}/N_{ATRP} \quad (7)$$

PMBTFVB–Br **3a** macroinitiator was employed to study the kinetics of bulk ATRP of St and the conversions of St were measured by GC as summarized in Table 3. The molecular weights increased with the raising of the conversions of St and the graft copolymers showed unimodal and symmetrical GPC curves in Fig. 6 with narrow molecular weight distributions ($M_w/M_n \leq 1.23$), which also matched the characteristics of ATRP. The semilogarithmic plot of Ln

Table 3
Kinetics studies of ATRP of St initiated by PMBTFVB–Br **3a**.^a

Sample	Time (h)	Conv. ^b (%)	M_n^c (kDa)	M_w/M_n^c
4i	1.5	2.33	11.4	1.21
4j	3.0	7.15	24.8	1.23
4k	5.0	10.03	31.9	1.23
4m	7.0	12.31	36.7	1.20

^a Polymerization temperature: 110 °C; feeding ratio: [St]:[CH₂Br group]:[CuBr]:[bpy] = 400:1:1:2; $V_{St}:V_{anisole} = 20:1$.

^b Determined by GC using anisole as internal standard.

^c Measured by GPC in THF at 35 °C.

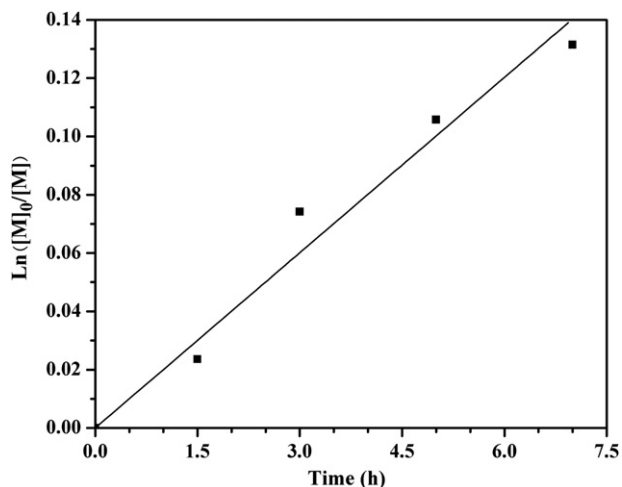


Fig. 8. Kinetic plots for bulk ATRP of styrene initiated by PMBTFVB–Br **3a** at 110 °C, [St]:[CH₂Br group]:[CuBr]:[bpy] = 400:1:1:2.

$\ln([M]_0/[M])$ vs. time is depicted in Fig. 8 on the basis of the data of conversions of St, which shows the conversion of St increases with the time and a linear dependence of $\ln([M]_0/[M])$ on the time when the feeding ratio of St to CH₂Br initiation group is 400:1. It is obvious that the apparent polymerization rate is first-order with respect to the concentration of St, illustrating a constant number of propagating species during the graft copolymerization of St. This phenomenon accorded with the characteristic of ATRP [31,32]. Thus, we can conclude that a series of PMBTFVB-g-PS **4** graft copolymers consisting of a PFCB aryl ether-based backbone possessing 31 repeating units and PS (15–53 repeating units per chain) side chains were successfully synthesized by the well-controlled ATRP of St initiated by PMBTFVB–Br **3** macroinitiator.

3.5. Properties of graft copolymer

Solubility tests were performed for PMBTFVB-g-PS **4** graft copolymers with different molecular weights in common solvents. These copolymers are soluble in most organic solvents such as THF, CH₂Cl₂, chloroform, acetone, ethyl acetate, toluene and DMF; however, it is insoluble in water and methanol.

Fig. 9 shows DSC thermogram of PMBTFVB-g-PS **4c** graft copolymer and two T_g s appeared at 100.9 °C and 85.8 °C, respectively. The higher T_g at 100.9 °C apparently corresponded to PS side chains, which was similar

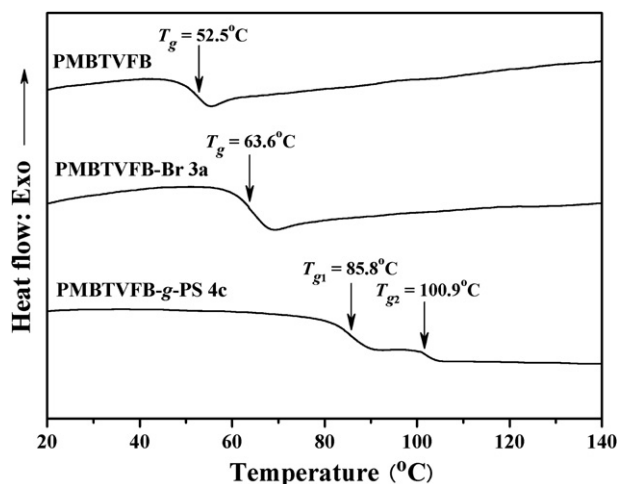


Fig. 9. Third heating DSC scans (in N₂) of PMBTFVB **2**, PMBTFVB–Br **3a**, and PMBTFVB–g-PS **4c** with a heating rate of 10 °C/min.

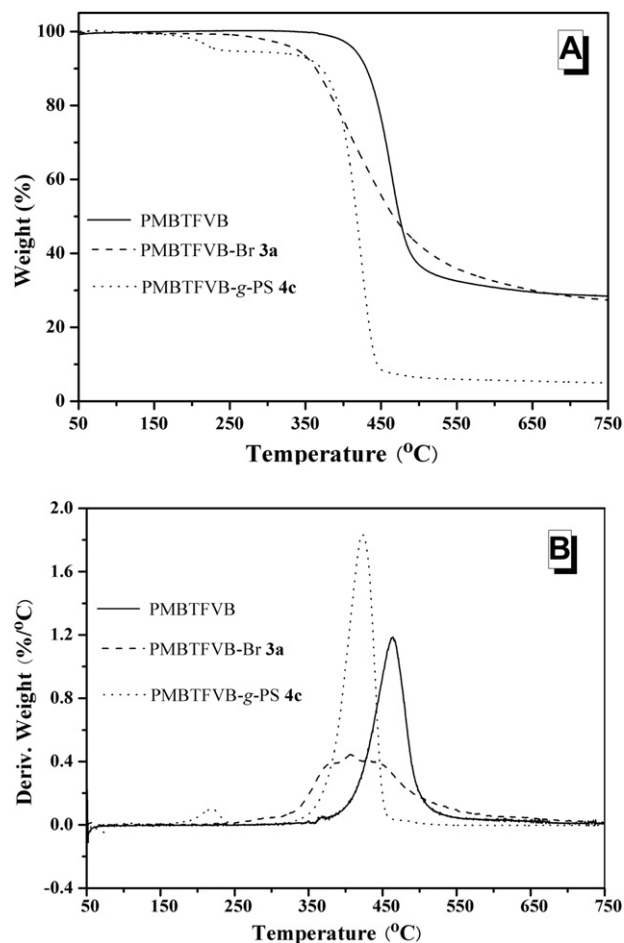


Fig. 10. TG (A) and DTG (B) curves (in N₂) of PMBTFVB **2**, PMBTFVB–Br **3a**, and PMBTFVB–g-PS **4c** with a heating rate of 10 °C/min.

to that of PS homopolymer [58]. The lower T_g at 85.8 °C was attributed to PMBTFVB backbone, which was much higher than those of PMBTFVB **2** homopolymer ($T_g = 52.5$ °C) and PMBTFVB–Br **3a** macroinitiator ($T_g = 63.6$ °C) as shown in Fig. 9; this can be explained that the free rotation of PMBTFVB backbone was confined by PS branches. The presence of two different T_g s also indicated a bulk microphase separation exist in PMBTFVB-g-PS **4** graft copolymer [59,60].

Thermal stability of the polymers was measured by TGA and the typical TG (thermogravimetry) and DTG (derivative thermogravimetry) curves are shown in Fig. 10. The pyrolysis of PMBTFVB **2** homopolymer and PMBTFVB–Br **3a** macroinitiator processed in a one-stage decomposition pattern and T_d of PMBTFVB **2** and PMBTFVB–Br **3a** is recorded at 431 °C and 364 °C respectively. However, the thermolysis of PMBTFVB-g-PS **4c** graft copolymer shows a two-step degradation process around about 221 °C and 425 °C, which corresponded to the weight loss of PS branches and PMBTFVB backbone, respectively.

4. Conclusions

In summary, a novel perfluorocyclobutyl aryl ether-based graft copolymer with relatively narrow molecular weight distributions ($M_w/M_n \leq 1.38$) was synthesized by the sequential thermal step-growth cycloaddition polymerization of 2-methyl-1,4-bis(trifluorovinyl)benzene and ATRP of styrene. The pendant methyls on the perfluorocyclobutyl aryl ether-based backbone were converted to ATRP initiation groups by NBS and BPO without affecting the main chain. The targeted graft copolymers were obtained by

the combination of the grafting-from strategy and ATRP of St. The polymerization showed a first-order kinetics and the molecular weight of the graft copolymer raised with the extending of the polymerization time. These fluoropolymers show excellent solubility in common organic solvent, which imply good processability.

Acknowledgement

The authors thank the financial support from National Natural Science Foundation of China (20674094, 21074145, 50873029, and 51073042), Shanghai Nano-Technology Program (0952nm05800), and Shanghai Rising Star Program (07QA14066).

References

- [1] Plunkett RJ. *Polym Prepr* 1986;27:485–7.
- [2] Babb DA, Snelgrove RV, Smith DW, Mudrich SF. Step-growth polymers for high-performance materials. Washington, DC: American Chemical Society; 1996. p. 431–41.
- [3] Kennedy AP, Babb DA, Bermmer JN, Pasztor AJ. *J Polym Sci Polym Chem* 1995;33:1859–65.
- [4] Babb DA, Ezzell BR, Clement KS, Richey WF, Kennedy AP. *J Polym Sci Polym Chem* 1993;31:3465–77.
- [5] Smith DW, Boone HW, Traiphol R, Shah H, Perahia D. *Macromolecules* 2000;33:1126–8.
- [6] Jin JY, Topping CM, Chen S, Ballato J, Foulger SH, Smith DW. *J Polym Sci Polym Chem* 2004;42:5292–300.
- [7] Ghim J, Shim HS, Shin BG, Park JH, Hwang JT, Chun C, et al. *Macromolecules* 2005;38:8278–84.
- [8] Choi WS, Harris FW. *Polymer* 2000;41:6213–21.
- [9] Huang XY, Wang RW, Zhao PQ, Lu GL, Zhang S, Qing FL. *Polymer* 2005;46:7590–7.
- [10] Smith DW, Chen S, Kumar SM, Ballato J, Topping C, Shah HV, et al. *Adv Mater* 2002;14:585–9.
- [11] Smith DW, Jin JY, Shah HV, Xie Y, DesMarteau DD. *Polymer* 2004;45:5755–60.
- [12] Wong S, Ma H, Jen AKY, Barto R, Frank CW. *Macromolecules* 2003;36:8001–7.
- [13] Ma H, Luo JD, Kang SH, Wong S, Kang JW, Jen AKY, et al. *Macromol Rapid Commun* 2004;25:1667–73.
- [14] Yoo MC, Chang BJ, Kim JH, Lee SB, Lee YT. *Memburein* 2005;15:355–62.
- [15] Liu S, Jiang X, Ma H, Liu MS, Jen AKY. *Macromolecules* 2000;33:3514–7.
- [16] Jiang X, Liu S, Liu MS, Herguth P, Jen AKY, Fong H, et al. *Adv Funct Mater* 2002;12:745–51.
- [17] Iacono ST, Budy SM, Ewald D, Smith DW. *Chem Commun*; 2006:4844–6.
- [18] Jin JY, Topping CM, Suresh S, Foulger SH, Rice N, Mojazza BH, et al. *Polymer* 2005;46:6923–32.
- [19] Jin JY, Smith DW, Topping CM, Suresh S, Chen S, Foulger SH, et al. *Macromolecules* 2003;36:9000–4.
- [20] Iacono ST, Budy SM, Mabry JM, Smith DW. *Polymer* 2007;48:4637–45.
- [21] Zhu YQ, Huang YG, Meng WD, Li HQ, Qing FL. *Polymer* 2006;47:6272–9.
- [22] Huang XY, Lu GL, Peng D, Zhang S, Qing FL. *Macromolecules* 2005;38:7299–305.
- [23] Lu GL, Zhang S, Huang XY. *J Polym Sci Polym Chem* 2006;44:5438–44.
- [24] Iacono ST, Budy SM, Marby JM, Smith DW. *Macromolecules* 2007;40:9517–22.
- [25] Zhang MF, Breiner T, Mori H, Müller AHE. *Polymer* 2003;44:1449–58.
- [26] Dziezok P, Sheiko SS, Fischer K, Schmidt M, Moller M. *Angew Chem Int Ed* 1997;36:2812–5.
- [27] Heroguez V, Gnanou Y, Fontanille M. *Macromolecules* 1997;30:4791–8.
- [28] Deffieux A, Schappacher M. *Macromolecules* 1999;32:1797–802.
- [29] Galal B, Durmaz H, Tasdelen MA, Hizal G, Tunca U, Yagci Y, et al. *Macromolecules* 2006;39:5330–6.
- [30] Beers KL, Gaynor SG, Matyjaszewski K, Sheiko SS, Moller M. *Macromolecules* 1998;31:9413–5.
- [31] Wang JS, Matyjaszewski K. *J Am Chem Soc* 1995;117:5614–5.
- [32] Wang JS, Matyjaszewski K. *Macromolecules* 1995;28:7901–10.
- [33] Matyjaszewski K, Xia JH. *Chem Rev* 2001;101:2921–90.
- [34] Oh JK, Min K, Matyjaszewski K. *Macromolecules* 2006;39:3161–7.
- [35] Jakubowski W, Matyjaszewski K. *Angew Chem Int Ed* 2006;45:4482–6.
- [36] Rosen BM, Percec V. *Chem Rev* 2009;109:5069–119.
- [37] Nguyen NH, Rosen BM, Lligadas G, Percec V. *Macromolecules* 2009;42:2379–86.
- [38] Moad G, Rizzardo E, Thang SH. *Acc Chem Res* 2008;41:1133–42.
- [39] Moad G, Rizzardo E, Thang SH. *Polymer* 2008;49:1079–131.
- [40] Hans M, Keul H, Heise A, Moeller M. *Macromolecules* 2007;40:8872–80.
- [41] Wang MF, Zou S, Guerin G, Shen L, Deng KQ, Jones M, et al. *Macromolecules* 2008;41:6993–7002.
- [42] Zhang YQ, Shen Z, Yang D, Feng C, Hu JH, Lu GL, et al. *Macromolecules* 2010;43:117–25.
- [43] Katsuhara Y, DesMarteau DD. *J Am Chem Soc* 1980;102:2681–6.
- [44] Resnick PR, Buck WH. In: Schirs J, editor. *Modern fluoropolymers: high performance polymers for diverse applications*. New York: Wiley; 1997. p. 397–420.
- [45] Neilson AR, Budy SM, Ballato JM, Smith DW. *Polymer* 2008;49:3228–32.
- [46] Jin JY, Smith DW, Glasser S, Perahia D, Foulger SH, Ballato J, et al. *Macromolecules* 2006;39:4646–9.
- [47] Peng D, Zhang XH, Huang XY. *Polymer* 2006;47:6072–80.
- [48] Peng D, Zhang XH, Feng C, Lu GL, Zhang S, Huang XY. *Polymer* 2007;48:5250–8.
- [49] Gu LN, Shen Z, Zhang S, Lu GL, Zhang XH, Huang XY. *Macromolecules* 2007;40:4486–93.
- [50] Liu SS, Ayusman S. *Macromolecules* 2000;33:5106–10.
- [51] Borner HG, Beers K, Matyjaszewski K. *Macromolecules* 2001;34:4375–83.
- [52] Cheng GL, Boker A, Zhang MF, Krausch G, Muller AHE. *Macromolecules* 2001;34:6883–8.
- [53] Matyjaszewski K, Qin SH, Boyce JR, Shirvanyants D, Sheiko SS. *Macromolecules* 2003;36:1843–9.
- [54] Shen Z, Chen Y, Barriau E, Frey H. *Macromol Chem Phys* 2006;207:57–64.
- [55] Peng D, Zhang XH, Huang XY. *Macromolecules* 2006;39:4945–7.
- [56] Peng D, Feng C, Lu GL, Zhang S, Zhang XH, Huang XY. *J Polym Sci Polym Chem* 2007;45:3687–97.
- [57] Jia ZF, Fu Q, Huang JL. *Macromolecules* 2006;39:5190–3.
- [58] Roland CM, Casalini R. *Macromolecules* 2005;38:8729–33.
- [59] Zhang XH, Shen Z, Li LT, Zhang S, Lu GL, Huang XY. *J Polym Sci Polym Chem* 2007;45:5509–17.
- [60] Zhang XH, Shen Z, Li LT, Lu GL, Gu LN, Huang XY. *Polymer* 2007;48:5507–13.